Research Square

Preprints are preliminary reports that have not undergone peer review.
They should not be considered conclusive, used to inform clinical practice,
or referenced by the media as validated information.

# Functional Analysis of SibHLH137 in Regulating Anthocyanin Biosynthesis and Drought Tolerance in Foxtail Millet

**Xin Yang**
Shanxi Normal University
**Minjing Kong**
Shanxi Normal University
**Li Zhang**
Shanxi Normal University
**Yajing Sun**
Shanxi Normal University
**Xiaoqian Fan**
Shanxi Normal University
**Meiping Zhang**
zhangmp2006@163.com

Shanxi Normal University https://orcid.org/0000-0003-0988-0158

**Research Article**

**Keywords:**

**Posted Date:** November 13th, 2026

**DOI:** https://doi.org/10.21203/rs.3.rs-10684856/v1

**License:** This work is licensed under a Creative Commons Attribution 4.0 International License.
Read Full License

# Functional Analysis of *SibHLH137* in Regulating Anthocyanin Biosynthesis and Drought Tolerance in Foxtail Millet

**Xin Yang[1†], Minjing Kong[1†], Li Zhang[1†], Yajing Sun[1], Xiaoqian Fan[1], Meiping Zhang[1*]**

[1] College of Life Sciences, ShanXi Normal University, Shanxi 030031, PR China
* Corresponding author. E-mail: zhangmp2006@163.com. Tel:+86-13835754160
† These authors contributed equally to this work.

**Abstract**

Drought is a major abiotic stress constraining the yield of foxtail millet (*Setaria italica* L.). Anthocyanins serve as natural antioxidants and play important roles in plant stress adaptation; however, their upstream transcriptional regulatory mechanisms remain unclear. In this study, we identified a bHLH transcription factor gene, *SibHLH137*, which exhibited significantly higher expression levels in various tissues of purple-leaf varieties than in green-leaf varieties. Heterologous over-expression of *SibHLH137* in *Arabidopsis* significantly promoted anthocyanin accumulation and upregulated the expression of late anthocyanin biosynthetic genes (*AtDFR, AtANS, AtUGT78D2*), and enhanced drought tolerance of transgenic plants by increasing proline content and antioxidant enzyme activities as well as upregulating drought-responsive genes (*AtRD29A, AtDREB2A*). To validate its function in foxtail millet, we established efficient regeneration and genetic transformation systems and obtained *SibHLH137*-overexpressing transgenic foxtail millet lines. Compared with wild-type plants, the transgenic lines exhibited darker caryopsis and stem coloration and significantly increased total anthocyanin content, with *SiDFR* expression upregulated by 30-fold. Under drought stress, the transgenic lines showed increased relative water content and proline content, reduced leaf water loss rate and malondialdehyde accumulation, enhanced antioxidant enzyme activities, and significant upregulation of drought-responsive genes including *SiDREB2*, *SiNCED1*, and *SiRAB18*. Promoter analysis revealed the presence of G-box elements in the promoter regions of target genes. Collectively, *SibHLH137* triggers anthocyanin biosynthesis and drought response pathways to improve drought resistance of foxtail millet, which offers valuable genetic resources for drought-resistance molecular breeding.

**Keywords:** Foxtail Millet; *SibHLH137*; anthocyanin; drought stress; genetic transformation

## 1. Introduction

Foxtail millet (*Setaria italica* L.) is an important minor cereal crop in northern China and has become a model plant for functional genomics studies in Poaceae, owing to its small genome size, short growth cycle, self-pollination, and $C_4$ photosynthetic pathway (Wu et al., 2018). It possesses a well-developed root system and high water use efficiency, conferring remarkable adaptability to drought and nutrient-poor environments. However, drought remains a major environmental constraint limiting its yield and quality (Wang et al., 2024; Hou et al., 2025).

Anthocyanins are a class of water-soluble flavonoid pigments that function as potent natural antioxidants. They play critical roles in plant adaptation to abiotic stress by scavenging excessive reactive oxygen species (ROS) induced by drought stress, regulating osmotic pressure, and enhancing photoprotection (Li et al., 2025; Hao et al., 2025; Prakash et al., 2026). The biosynthesis of anthocyanins is finely regulated by the MYB-bHLH-WD40 (MBW) transcriptional complex (Zhang et al., 2026). In recent years, increasing attention has been paid to the dual functions of bHLH transcription factors in integrating anthocyanin metabolism and stress responses. For instance, in *Chaenomeles speciosa*, drought stress-induced *CsbHLH111* interacts with *CsMYB123* to cooperatively activate anthocyanin biosynthetic genes including CsCHI, CsDFR, and CsANS, thereby promoting anthocyanin accumulation (Ding et al., 2025; Wang et al., 2026). Similarly, in *Glycyrrhiza uralensis, GubHLH38* and *GubHLH64* have been confirmed to be closely associated with anthocyanin biosynthesis under abiotic stress conditions (Lira et al., 2017). However, how bHLH transcription factors regulate anthocyanin accumulation

and participate in drought stress responses in foxtail millet remains largely unclear.

In this study, we first preliminarily validated the basic functions of *SibHLH137* in regulating anthocyanin biosynthesis and drought tolerance through heterologous over-expression in *Arabidopsis.* On this basis, we established an efficient genetic transformation system for foxtail millet and obtained stable transgenic lines over-expressing *SibHLH137*. Through drought stress treatment combined with physiological and biochemical measurements, gene expression analysis, and promoter cis-acting element dissection, we systematically investigated the dual functions of *SibHLH137* in anthocyanin accumulation and drought stress responses in foxtail millet, as well as its underlying molecular regulatory mechanisms, aiming to provide genetic resources and a theoretical basis for drought-resistant molecular breeding in foxtail millet.

## 2. Materials and Methods

### 2.1 Plant Materials and Growth Conditions

The plant materials included foxtail millet varieties Heizhigu, Heigu, Xiaoheigu, Jingu 21 and CC431, as well as wild-type *Arabidopsis thaliana* ecotype Col-0. The foxtail millet varieties were provided by the Laboratory of Characteristic Cereal Physiology and Ecology, College of Life Sciences, Shanxi Normal University. Foxtail millet seeds were surface-sterilized and sown in nutrient soil, then placed in an artificial climate chamber under the following conditions: 16 h light (28°C)/8 h dark (23°C) with a light intensity of 10,000 Lx. *Arabidopsis* seeds were vernalized at 4°C for 3 d and then sown on MS medium or nutrient soil, and grown in a culture room at 22°C with a photoperiod of 16 h light/8 h dark.

### 2.2 Vector Construction and *Arabidopsis* Genetic Transformation

The coding sequence of *SibHLH137* was amplified from cDNA of Heigu and cloned into the pCAMBIA1300 vector via homologous recombination to generate the over-expression construct pCAMBIA1300-SibHLH137. The recombinant plasmid was then transformed into Agrobacterium tumefaciens strain GV3101. *Arabidopsis* transformation was performed using the floral dip method. Transgenic plants were selected on medium containing 25 mg/L hygromycin and further self-pollinated to obtain homozygous $T_3$ generation lines. Positive transgenic plants were identified by PCR and qRT-PCR analysis (Song et al., 2019).

### 2.3 Establishment of the Foxtail Millet Regeneration System and Genetic Transformation

Mature embryos of four foxtail millet varieties were used as explants and cultured on CIM3 induction medium (MS supplemented with 2.0 mg/L 2,4-D and 0.5 mg/L KT plus 100 mg/L activated charcoal) in darkness for 30 days to induce callus formation. Compact embryogenic calli were subcultured onto SIM1 differentiation medium (MS + 0.5 mg/L 6-BA + 0.1 mg/L NAA) and incubated at 28 °C under a 16 h light / 8 h dark photoperiod for 4–5 weeks to induce adventitious shoots. Adventitious shoots with a length of 2–3 cm were excised and transferred to half-strength MS medium containing 0.1 mg/L NAA for root induction.Meanwhile, a shoot-tip regeneration system was established. Foxtail millet seeds were incubated on moist filter paper under dark conditions for 5 days, after which tender shoot tips were isolated and inoculated on MS proliferation medium supplemented with 0.5 mg/L 6-BA and 0.1 mg/L NAA for the propagation of clustered shoots. The proliferated plantlets were then moved to the same half-strength MS rooting medium with 0.1 mg/L NAA to develop roots, which drastically shortened the whole plant regeneration cycle.

Embryogenic calli induced from mature embryos of CC431 were used as explants for Agrobacterium-mediated genetic transformation. Activated Agrobacterium suspension was adjusted to an $OD_{600}$ value of 0.6, and the calli were immersed in SCM suspension medium with shaking for 20 min. After infection, the calli were cultured on CM medium in darkness at 22 °C for 2 days of co-cultivation, then rinsed repeatedly with sterile water containing cefotaxime and air-dried. Subsequently, the treated calli were transferred to DSM differentiation screening medium supplemented with 25 mg/L Hygromycin and 100 mg/L Timentin to induce resistant adventitious shoots. Shoots reaching 2-3 cm in length were excised and transferred to RSM rooting screening medium for 2-3 weeks of subculture. Rooted plantlets were uncovered and acclimatized under humid conditions for 2 days before transplantation. Leaf tissues were collected from surviving $T_0$ regenerants, and positive transgenic lines were identified by PCR, RT-PCR and qRT-PCR.

2.4 Physiological and Biochemical Parameter Assays

Total anthocyanin content was determined using the 1% hydrochloric acid-methanol method (Huang et al., 2019). Relative water content was measured according to Zhang et al. (2026), and leaf water loss rate was determined as described by Liu et al. (2026). Proline content was assayed using the method of Li et al. (2022), and malondialdehyde (MDA) content was measured following Cui et al. (2023). The activities of superoxide dismutase (SOD), catalase (CAT), and peroxidase (POD) were assayed according to Liang et al. (2026). Histochemical staining with DAB and NBT was performed to visualize the accumulation of $H_2O_2$ and $O_2^-$, respectively (Jiang et al., 2026).

2.5 Physiological and Biochemical Parameter Assays

The expression levels of anthocyanin biosynthesis-related genes (*CHS*, *CHI*, *DFR*, and *ANS*) and drought-responsive genes (*DREB2*, *NCED1*, *RAB18*, *LEA14*, etc.) were detected by qRT-PCR, with *SiACTIN* serving as the internal reference gene. The primer sequences are listed in Supplementary Table S4.

2.6 Promoter Cis-Acting Element Analysis

The promoter sequences (1,500-2,000 bp upstream of the start codon) of target genes were analyzed using the online software PlantCARE, with particular focus on the distribution of G-box (CACGTG) and its variants (Ren et al., 2023).

## 3. Results

3.1 Analysis of Bioinformatic Characteristics and Expression Patterns of *SibHLH137*

3.1.1 Bioinformatic Analysis of *SibHLH137*

To elucidate the molecular characteristics of *SibHLH137*, bioinformatics prediction was performed on its gene sequence and encoded protein. The *SibHLH137* gene contains a 921 bp open reading frame (Figure 1A). Secondary structure prediction revealed that the SibHLH137 protein is predominantly composed of random coils, consisting of 188 amino acids accounting for 62.05%, followed by α-helices composed of 109 amino acids accounting for 35.97%, and extended strands composed of 6 amino acids accounting for 1.98% (Figure 1B).

3.1.2 Analysis of *SibHLH137* Expression Characteristics and Its Role in Drought-Induced Anthocyanin Accumulation

Three green-leaf foxtail millet varieties, Jingu 21 (G1), Changsheng 07 (G2), and Qinzhouhuang (G3), and three purple-leaf varieties, Heizhigu (P1), Heigu (P2), and Xiaoheigu (P3), were used as experimental materials. Quantitative anthocyanin detection results (Figure 1C) showed that under normal conditions, green leaves had almost no anthocyanin accumulation, whereas purple-leaf varieties exhibited higher pigment content. After drought treatment, anthocyanin content increased in all varieties, with only 1.34- to 1.93-fold increases in green-leaf varieties and 2.18- to 2.69-fold increases in purple-leaf varieties.

To examine the tissue-specific expression pattern of *SibHLH137*, we selected Jingu 21 (green) and Heigu (purple), which showed the most pronounced differences in anthocyanin phenotype. qRT-PCR results revealed that the gene was expressed in roots, stems, leaves, and seeds, with the highest expression level in seeds. Moreover, in each corresponding tissue, the expression level of *SibHLH137* in the purple variety P2 was significantly higher than that in the green variety G1, suggesting that high expression of *SibHLH137* is closely associated with anthocyanin accumulation and drought-induced pigment synthesis in foxtail millet (Figure 1D).

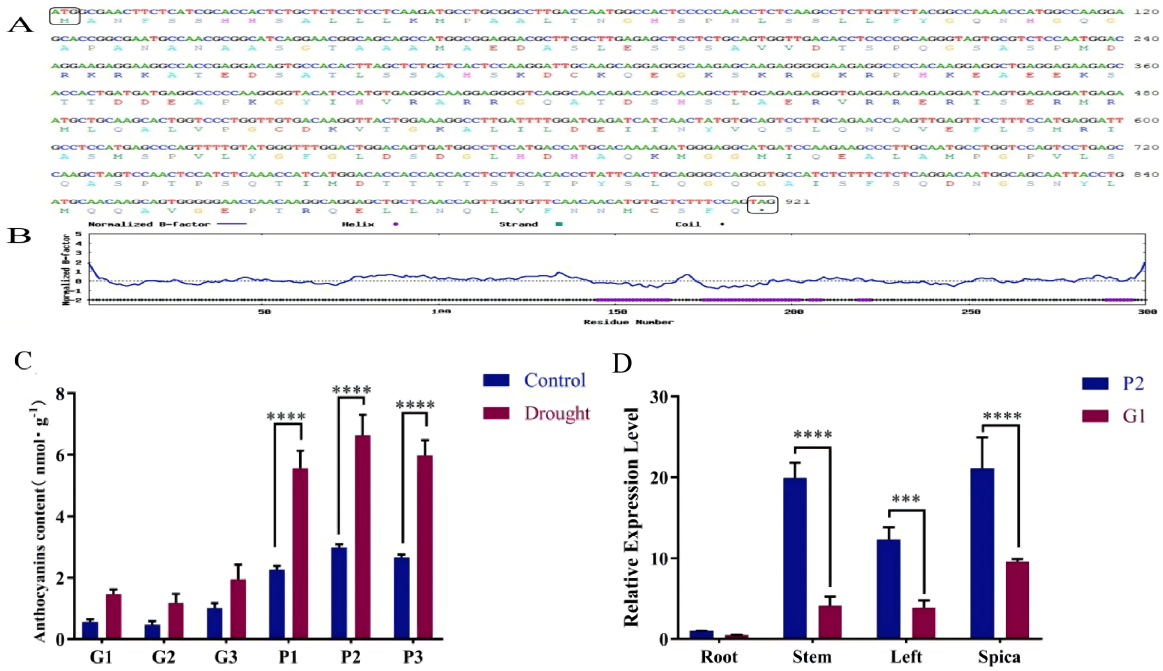



**Figure 1.** Bioinformatic analysis and expression pattern of *SibHLH137*. (A)Nucleotide sequence of *SibHLH137* gene; (B)Secondary structure diagram of *SibHLH137* protein; (C)Determination of anthocyanin content in different foxtail millet accessions under control and drought conditions; (D)Relative expression levels of *SibHLH137* in different tissues (root, stem, leaf, spica) of G1 and P2 foxtail millet.

### 3.2 Over-expression of *SibHLH137* Promotes Anthocyanin Accumulation and Drought Tolerance in *Arabidopsis*

#### 3.2.1 Generation of Homozygous *SibHLH137*-Overexpressing *Arabidopsis* Lines

To investigate the biological function of *SibHLH137*, the *SibHLH137* gene was amplified from Heigu cDNA as template (Figure 2A), and the pCAMBIA1300-SibHLH137 over-expression vector was constructed. The correctness of the construct was verified by colony PCR and Agrobacterium liquid culture PCR (Figures 2B, C). The recombinant plasmid was introduced into wild-type *Arabidopsis* (Col-0) via Agrobacterium-mediated floral dip method, and transgenic lines were obtained by hygromycin screening. Homozygous $T_3$ generation lines were identified (Figure 2D). The $T_3$ plants were subjected to PCR verification, and the target band of approximately 963 bp was detected as expected (Figure 2E). Three *SibHLH137* transgenic lines (OE-1/2/3) were selected, and RT-PCR analysis confirmed the integration of *SibHLH137* in transgenic *Arabidopsis*, while no expression of *SibHLH137* was detected in wild-type plants (Figure 2F). qRT-PCR analysis further confirmed that the expression levels of *SibHLH137* in OE-1/2/3 transgenic lines were all higher than that in wild type, indicating successful genetic transformation (Figure 2G).

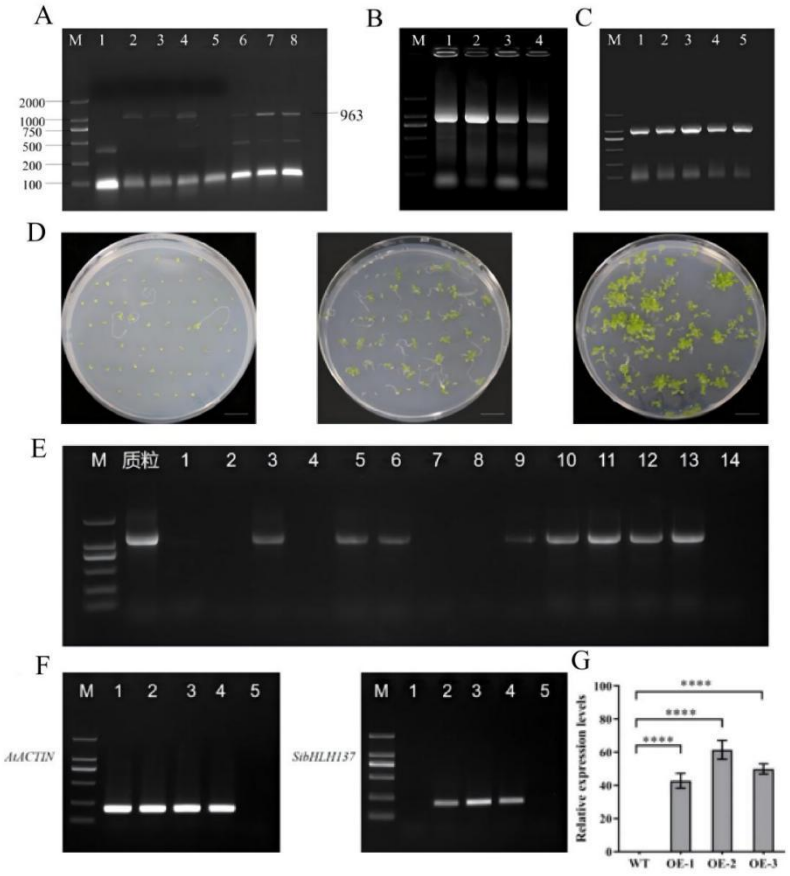



**Figure 2.** Construction and molecular identification of SibHLH137-overexpressing *Arabidopsis* lines. (A-C)Construction of pCAMBIA1300-SibHLH137 over-expression vector. (A)Amplification of *SibHLH137* sequence; (B)Electrophoresis of colony PCR verification; (C)PCR identification of Agrobacterium tumefaciens. (D-G)Transformation of pCAMBIA1300-SibHLH137 into *Arabidopsis*. (D)Positive selection, scale bars represent 1 cm; (E)Target gene detection; (F)RT-PCR detection of *SibHLH137* in over-expression *Arabidopsis*; (G)qRT-PCR detection of *SibHLH137* in over-expression *Arabidopsis*. Asterisks indicate significant differences based on two-way ANOVA (****, $P$<0.0001).

### 3.2.2 Over-expression of *SibHLH137* Promotes Anthocyanin Accumulation in *Arabidopsis*

During the growth of wild-type and SibHLH137 transgenic *Arabidopsis*, the effect of SibHLH137 on anthocyanin accumulation was observed. Under normal growth conditions, SibHLH137 over-expression lines exhibited obvious purple pigmentation in lateral branches, stem apices, stigmas, and leaves compared with wild-type plants. After drought treatment, the leaves of transgenic *Arabidopsis* turned purple following chlorophyll degradation, whereas wild-type leaves turned yellow and withered. The whole-plant anthocyanin extracts also showed color differences between wild-type and transgenic *Arabidopsis*, with the wild-type extract being colorless and transparent, while the transgenic extract appeared light purple.

Based on the above phenotypes, the total anthocyanin content and the relative transcript levels of anthocyanin biosynthesis-related genes (*AtCHI*, *AtCHS*, *AtF3H*, *AtF3'H*, *AtDFR*, *AtANS*, and *AtUGT78D2*) were determined in wild-type and *SibHLH137* transgenic *Arabidopsis* whole plants. The results showed that the total anthocyanin content of *SibHLH137* transgenic *Arabidopsis* was significantly higher than that of wild type, which was consistent with the phenotypic observations. In the over-expression lines, the transcript levels of the early anthocyanin biosynthetic genes *AtCHS* and *AtCHI* were slightly higher than those in wild type, but the differences were not statistically significant. In contrast, the transcript levels of the late biosynthetic genes *AtF3H*, *AtF3'H*, *AtDFR*, *AtANS*, and *AtUGT78D2* were significantly up-regulated. Among them, the expression levels of *AtDFR* and *AtANS* were approximately 30-fold higher than those in wild type, and AtUGT78D2 was approximately 40-fold higher. These results indicated that *SibHLH137* promotes anthocyanin accumulation in *Arabidopsis* by up-regulating the expression of late anthocyanin biosynthetic genes.

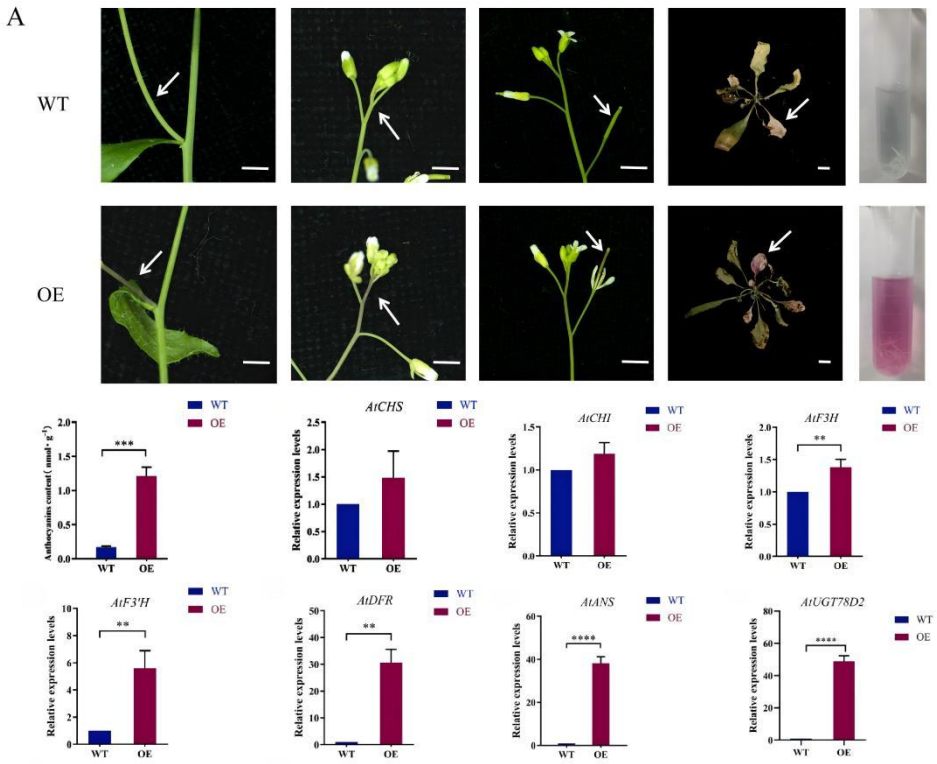



**Figure 3.** Over-expression of SibHLH137 promotes anthocyanin accumulation in *Arabidopsis*. (A)Phenotypes of anthocyanin accumulation in wild-type and transgenic *Arabidopsis*. The scale bar represents 1 cm. The centrifuge tubes on the right show the anthocyanin extracts from whole plants; (B)Anthocyanin content; (C-I)Relative expression levels of AtCHI (C), *AtCHS* (D), *AtF3H* (E), *AtF3'H* (F), *AtDFR* (G), *AtANS* (H) and *AtUGT78D2* (I). Asterisks indicate sienificant differences based T test(**, $p$<0.01; ***, $p$<0.001; ****, $p$<0.0001)

### 3.2.3 Over-expression of SibHLH137 Enhances Drought Stress Tolerance in *Arabidopsis*

#### 3.2.3.1 Over-expression of SibHLH137 Enhances Drought Tolerance of *Arabidopsis* at Germination and Seedling Stages

To evaluate the function of *SibHLH137* in drought stress responses, mannitol was used to mimic osmotic stress, and the growth performance of wild-type and SibHLH137-overexpressing *Arabidopsis* during seed germination was compared. Under normal conditions, no significant difference was observed between wild-type and transgenic plants, with germination rates close to 100%. As mannitol concentration increased, germination was progressively inhibited in all lines, with over-expression lines consistently showing milder inhibition than wild type. At 300 mM mannitol, the germination rate of wild type was only 54.3%, whereas those of OE-1, OE-2, and OE-3 reached 72.6%, 67.3%, and 71.0%, respectively, with a few plants still retaining green cotyledons (Figures 4A, B). Root length measurement under mannitol stress showed that transgenic *Arabidopsis* had longer average root length than wild type on 0 mM mannitol MS medium, with no significant difference in fresh weight. With increasing mannitol concentrations, root elongation was inhibited in both genotypes, but wild-type plants displayed more severe inhibition and greater fresh weight reduction. At 200 mM mannitol, root length of wild type decreased by 1.60 cm on average compared with the control, while those of OE-1, OE-2, and OE-3 decreased by 1.16 cm, 1.30 cm, and 1.20 cm, respectively, with both root length and fresh weight of over-expression lines significantly exceeding those of wild type (Figure 4C). After 10 days of natural drought treatment at the seedling stage, wild-type plants exhibited severe wilting or even death, whereas over-expression lines remained largely green with only partial leaf yellowing. Following rewatering, the survival rates of over-expression lines ranged from 85% to 95%, significantly higher than that of wild type (13.33%) (Figure 4D).

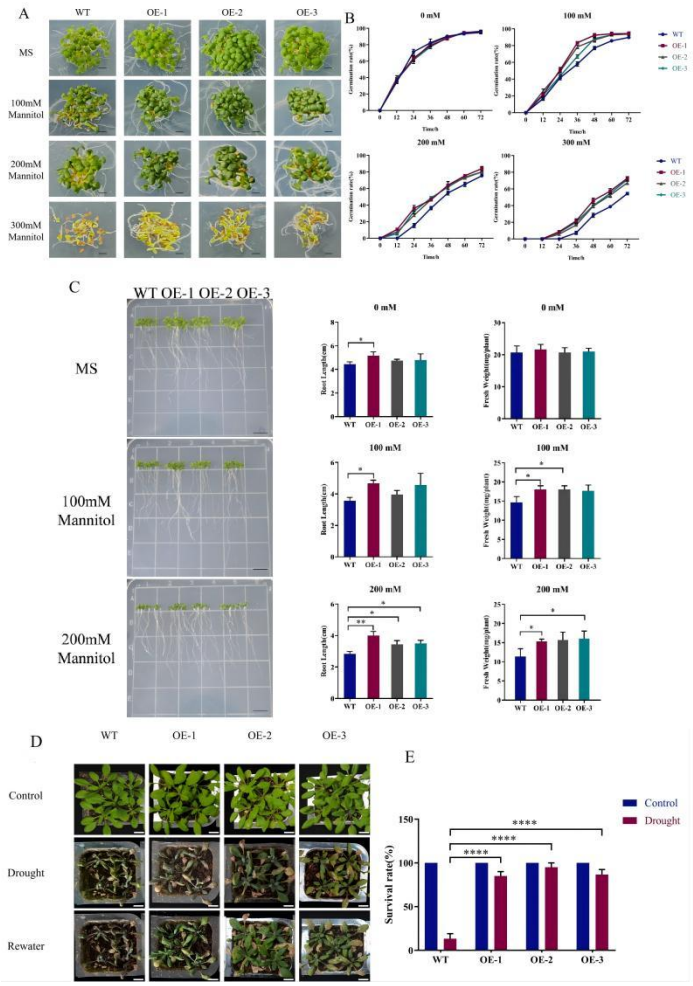



**Figure 4.** Phenotypic analysis of SibHLH137-overexpressing Arabidopsis under osmotic stress and drought stress. (A)Germination phenotypes of wild-type and over-expression lines on media with different mannitol concentrations; (B)Germination rates of the plants shown in (A); (C)Root length and fresh weight measurements of the plants shown in (A); (D)Growth phenotypes of wild-type and transgenic *Arabidopsis* under natural drought treatment; (E)Water recovery survival rates of the plants shown in (D). Scale bars represent 1 cm. Asterisks indicate significant differences based on two-way ANOVA (*， $p$<0.05; **， $p$<0.01; ****, $P$<0.0001).

3.2.3.2 Over-expression of *SibHLH137* Enhances Osmotic Regulation and Antioxidant Capacity of *Arabidopsis* under Drought Stress

To elucidate the physiological basis of *SibHLH137*-enhanced drought tolerance, ROS accumulation, stomatal movement, and osmotic regulation parameters were examined in wild-type and over-expression lines under drought stress. DAB and trypan blue staining revealed that wild-type leaves exhibited darker brown and blue coloration with significantly larger stained areas than over-expression lines after drought treatment, indicating greater $H_2O_2$ accumulation and more severe cell death in wild-type plants, whereas *SibHLH137* over-expression effectively alleviated oxidative damage and cell death (Figure 5A). Stomatal movement analysis showed that both stomatal width and area were significantly smaller in over-expression lines than in wild type under drought stress, suggesting that *SibHLH137* may reduce water loss by promoting stomatal closure to lower transpiration rate (Figure 5B).

After 10 days of drought treatment, relative water content, proline content, MDA content, chlorophyll content, and antioxidant enzyme activities were measured in leaves. Over-expression lines exhibited significantly higher relative water content and proline content, but lower MDA content than wild type, indicating that *SibHLH137* over-expression favored water balance maintenance, osmotic regulatory substance accumulation, and alleviation of membrane lipid peroxidation. Under control conditions, no significant differences were observed in chlorophyll content, SOD activity, or CAT activity between wild type and OE lines. After drought treatment, chlorophyll content and CAT activity were significantly elevated

in over-expression lines, whereas SOD activity showed no significant difference (Figure 5C).

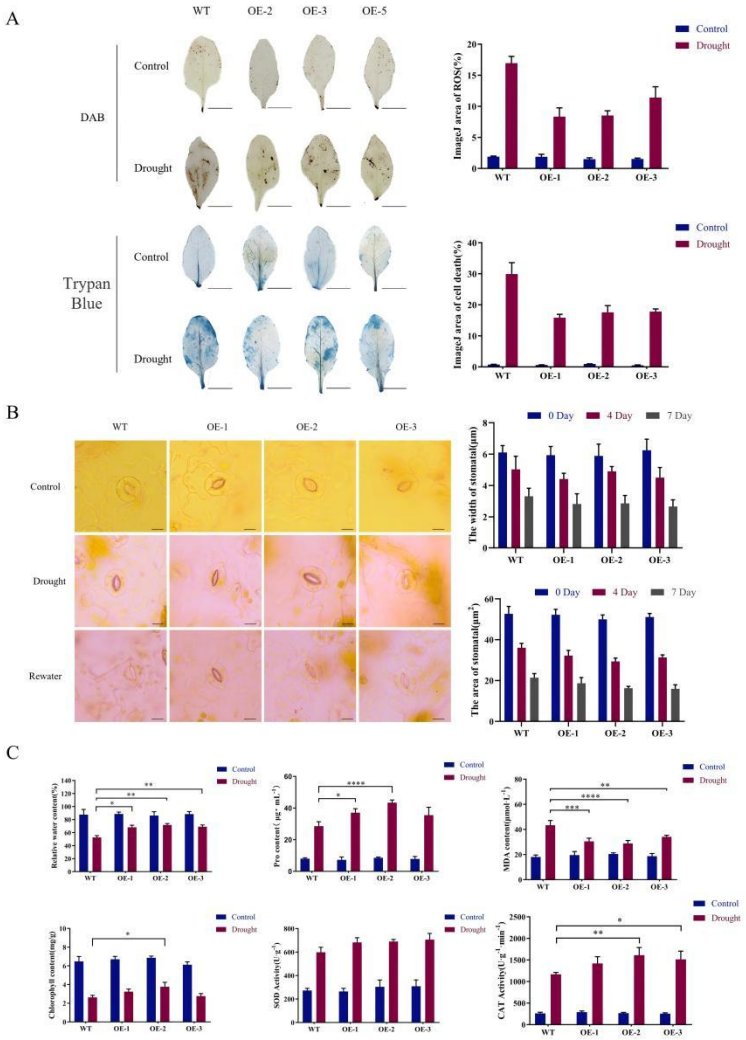



**Figure 5.** Analysis of ROS accumulation, stomatal movement and physiological parameters in *SibHLH137*-overexpressing *Arabidopsis* under drought stress. (A)Detection of $H_2O_2$ accumulation in leaves by DAB staining (upper) and cell death in leaves by trypan blue staining (lower), scale bars represent 1 cm; (B)Stomatal aperture analysis, scale bars represent 10 μm; (C)Determination of relative water content, proline content, malondialdehyde content, chlorophyll content, superoxide dismutase activity and catalase activity. Asterisks indicate significant differences based on two-way ANOVA (*, $p$<0.05; **, $p$<0.01; ***, $P$<0.001; ****, $P$<0.0001).

3.2.3.3 Over-expression of *SibHLH137* Upregulates the Expression of Drought Stress-Responsive Genes

To further investigate the molecular mechanism by which *SibHLH137* regulates the response to drought stress, the relative transcript levels of drought stress-responsive genes (*AtDREB2A*, *AtRD29A*, *AtRD29B*, *AtRD22*, *AtRAB18*, and *AtABI2*) were examined by qRT-PCR in wild-type and *SibHLH137* transgenic *Arabidopsis*. Under normal growth conditions, no significant differences were observed in the expression levels of these six genes between wild-type and over-expression lines. After drought treatment, the transcript levels of all six genes were significantly higher in OE-1, OE-2, and OE-3 than in wild type (Figure 6). Notably, since *AtRAB18* and *AtABI2* are genes involved in the ABA signaling pathway, it is suggested that *SibHLH137* may participate in the ABA signaling pathway to mediate drought stress responses.

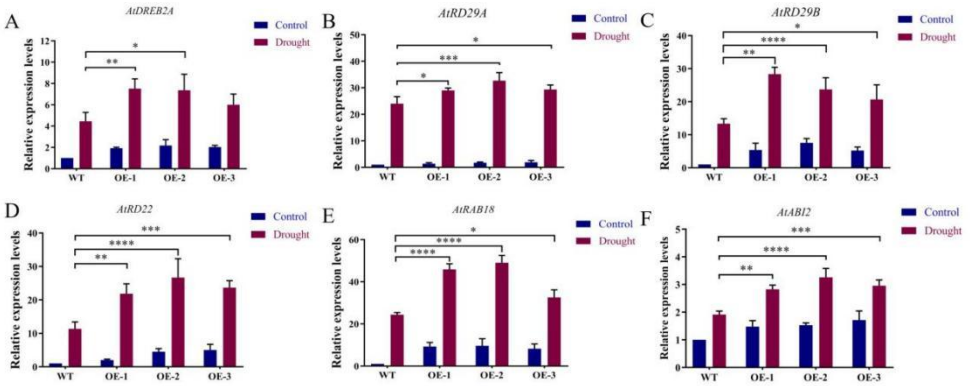



**Figure 6.** Relative expression levels of drought-stress response genes. (A-F)Relative expression levels of *AtDREB2A* (A), *AtRD29A* (B), *AtRD29B* (C), *AtRD22* (D), *AtRAB18* (E) and *AtABI2* (F). Asterisks indicate significant differences based on two-way ANOVA (*, $p<0.05$; **, $p<0.01$; ***, $P<0.001$; ****, $P<0.0001$).

### 3.3 Generation of *SibHLH137*-Overexpressing Transgenic Foxtail Millet Lines

#### 3.3.1 Establishment of an Efficient Regeneration System for Foxtail Millet

To establish an efficient recipient system for genetic transformation, mature embryos from four foxtail millet accessions were used as explants to screen suitable regeneration genotypes and medium combinations. CC431 was identified as the optimal genotype, with a callus induction rate of 91.97% on CIM3 medium (MS + 2.0 mg/L 2,4-D + 0.5 mg/L KT + 100 mg/L activated charcoal). Among the four varieties, CC431 exhibited the highest average induction rate of 61.62%, significantly outperforming Heigu, Heizhigu, and Xiaoheigu (Figure S1A; Table S1). SIM1 medium (MS + 0.5 mg/L 6-BA + 0.1 mg/L NAA) gave the highest differentiation rate of 65.0%, which decreased with increasing 6-BA concentration (Figure S1B; Table S2). The optimal rooting medium was 1/2 MS + 0.1 mg/L NAA, achieving a rooting rate of 93.33% and significantly promoting root elongation (Figures S1C, D).Using the optimized media, a complete in vitro regeneration protocol for CC431 mature embryos was established (Figure 8). Mature embryos inoculated on induction medium formed yellowish, compact calli after 30 d (Figures 7A, B). After subculture, the calli developed into granular, bright embryogenic calli (Figure 7C). Upon transfer to differentiation medium, green shoot primordia appeared after 1 week (Figure 7D) and developed into adventitious shoots after 2 weeks (Figure 7E). The shoots were rooted on 1/2 MS medium with 0.1 mg/L NAA (Figures 7F, G) and transplanted to soil after hardening, yielding complete regenerated plants (Figures 7H, I).

Additionally, a rapid shoot tip regeneration system was established (Figure 8). Shoot tips from seeds germinated on moist filter paper for 3-4 d were cultured on proliferation medium, where green primordial structures appeared after 3d (Figure 8C) and complete shoots formed after 1 week (Figure 8D). Shoot elongation and clustered shoot proliferation were promoted after subculture (Figure 8E), and roots developed on 1/2 MS medium (Figure 8F). The entire cycle from sowing to complete plant regeneration took less than 2 months, significantly shortening the regeneration period (Figure 8G).

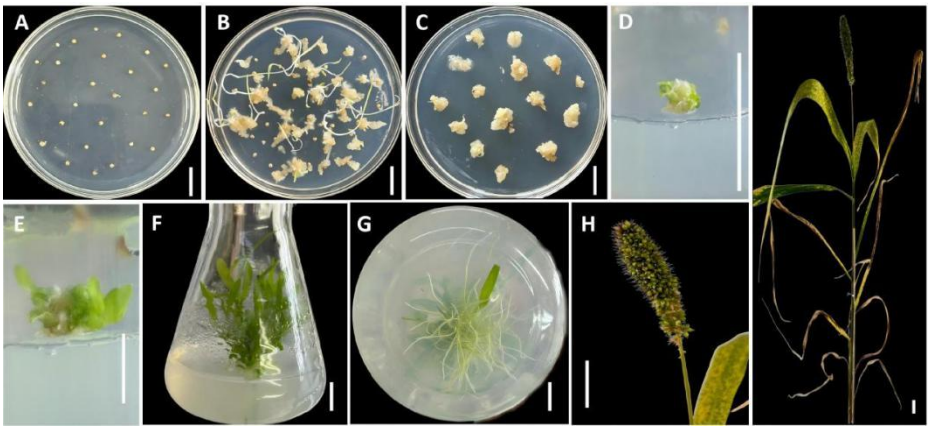



**Figure 7.** The Procedure for the Callus Regeneration System of Foxtail Millet Variety CC431. (A)Mature embryos inoculated on induction medium. (B)Callus induced after 30d of culture. (C)Embryogenic callus subcultured for one week on maintenance medium. (D)Green shoot

primordia appearing after 7d on differentiation medium. (E) Cluster shoots formed after 14 d on differentiation medium. (F-G) Rooting of cluster shoots on rooting medium. (H-I) Regenerated plants and young panicles after 60d of growth in potting soil. Scale bars represent 2 cm.

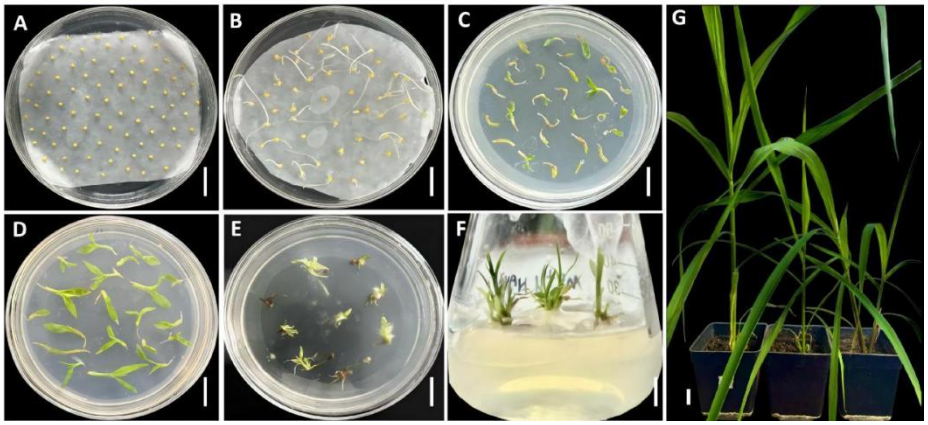



**Figure 8.** Establishment of the foxtail millet shoot tip regeneration system. (A)Dehulled mature embryos on moist filter paper. (B)Shoot tips of foxtail millet after 3d of culture at room temperature. (C)Shoot tips cultured on proliferation medium for 3d. (D)Shoot tips cultured on proliferation medium for 7d. (E)Shoot tips cultured on proliferation medium for 14d. (F)Regenerated plantlets on 1/2 MS medium. (G)Regenerated plants after 4 weeks of growth in potting soil. Scale bars represent 2 cm.

### 3.3.2 Establishment of an Efficient Genetic Transformation System for Foxtail Millet

Using *SibHLH137* as the target gene, genetic transformation was performed via the Agrobacterium-mediated method. High-quality calli obtained after one round of subculture were used as the transformation recipients. After Agrobacterium infection, the calli were co-cultivated for 2d and then transferred to selection medium for resistance screening. Because the transformation vector carries a hygromycin resistance gene, transformed cells were able to normally induce shoot formation on DSM differentiation medium containing hygromycin, while untransformed cells turned brown and died due to lack of resistance. The resistant shoots were transferred to RSM rooting medium for further culture, where untransformed shoots gradually turned yellow and died, whereas transformed shoots rooted normally. When roots reached 4-6 cm in length, the regenerated plants were transplanted into pots for continued growth (Figure 9).

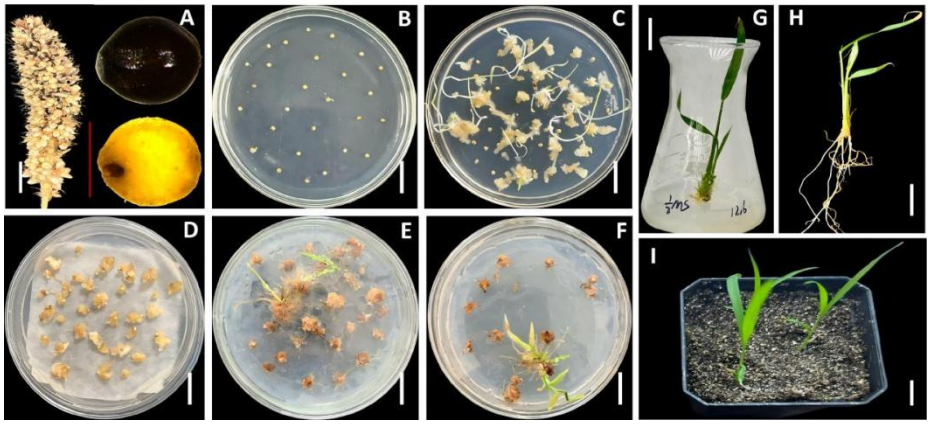



**Figure 9.** Genetic transformation of *SibHLH137*. (A)Panicles, unhulled mature seeds, and dehulled mature seeds of CC431. (B)Mature embryos inoculated on induction medium. (C)Calli induced on induction medium after 45d of culture. (D)Calli co-cultivated with Agrobacterium for 2d. (E)Shoots selected on screening medium. (F-H) Rooting of selected shoots on rooting screening medium. (I)Regenerated plantlets transplanted into potting soil. White scale bars represent 2 cm, red scale bars represent 2 mm.

### 3.3.3 DNA-Level Detection of *SibHLH137*-Overexpressing Foxtail Millet Lines

To identify the positive status of the transgene in $T_0$ generation foxtail millet plants, genomic DNA was extracted from five vigorously growing $T_0$ regenerated seedlings and one wild-type (WT) control plant using the CTAB method. Using the plant DNA as template, the over-expression vector sequence (*SibHLH137*-F1/R1) was amplified. Successful amplification of the corresponding sequence indicated that the surviving plants had been successfully transformed with the *SibHLH137* over-expression construct. Electrophoresis results (Figure 11) showed that among the five $T_0$ transgenic plants tested, four

(OE1, OE3, OE4, and OE5) exhibited a specific target band of approximately 963 bp, consistent with the expected fragment size, while no amplification band was detected in the wild-type (WT) control at the corresponding position (Figure 10A). RT-PCR analysis of the four *SibHLH137* transgenic lines (OE1, OE3, OE4, and OE5) detected the target band in both wild-type and transgenic plants, with brighter bands observed in the transgenic lines compared to wild type (Figure 10B). qRT-PCR further confirmed that the expression levels of *SibHLH137* in OE1, OE3, OE4, and OE5 were all higher than those in wild type (Figure 10C). These results indicated that *SibHLH137*-overexpressing transgenic foxtail millet lines were successfully obtained for subsequent gene function studies.

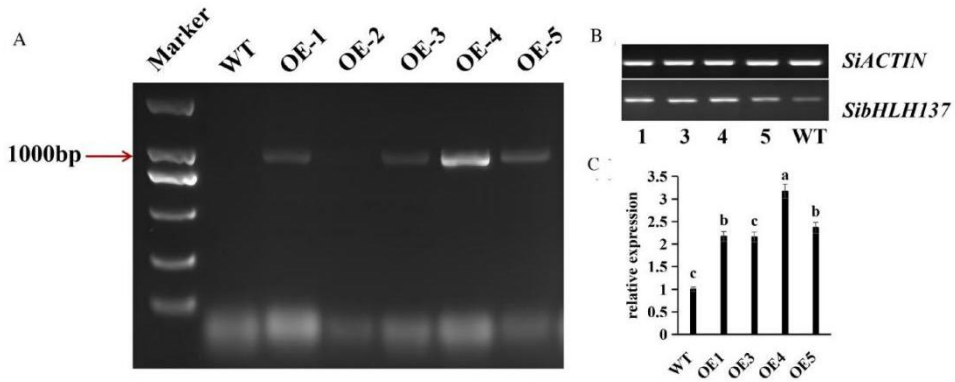



**Figure 10.** PCR identification of transgenic foxtail millet. (A)Detection of the target gene by PCR. (B)RT-PCR positive detection of SibHLH137-overexpressing foxtail millet. (C)qRT-PCR positive detection of *SibHLH137*-overexpressing foxtail millet. Different lowercase letters indicate significant differences ($P < 0.05$).

### 3.4 Over-expression of *SibHLH137* Promotes Anthocyanin Accumulation in Foxtail Millet

To investigate the regulatory function of *SibHLH137* in anthocyanin biosynthesis in foxtail millet, the grain and vegetative organ phenotypes of wild-type (WT) and over-expression transgenic lines were examined. Under unhulled conditions, no obvious difference in seed coat color was observed among the lines; however, after dehulling, the caryopsis color of over-expression lines was significantly darker (deep brown) compared to the yellowish-brown WT caryopsis (Figure 11A). Phenotypic observation of vegetative organs revealed that over-expression lines (OE1, OE3) exhibited obvious purple pigmentation in stems under normal growth conditions, whereas WT stems were green or only slightly purple (Figure 11B). To verify the correlation between these phenotypic differences and anthocyanin accumulation, total anthocyanins were extracted from WT, OE1, and OE3 plants for quantitative analysis. The extracts from over-expression lines displayed a darker purplish-red color (Figure 11C). $OD_{530}$ absorbance measurements showed that total anthocyanin contents in OE1 and OE3 were 2.2-fold and 2.5-fold higher than those in WT, respectively, with both differences reaching statistical significance ($P < 0.05$) (Figure 11D). Furthermore, qRT-PCR was performed to examine the expression levels of key genes in the anthocyanin biosynthetic pathway before and after drought stress. Under normal growth conditions, the transcript levels of *SiCHS*, *SiCHI*, *SiDFR*, and *SiANS* were all significantly higher in over-expression lines than in WT, with *SiDFR* expression reaching 30-fold that of WT ($P < 0.05$). After drought stress, the induction levels of these four genes were greater in over-expression lines than in WT (Figure 11E). Collectively, these results indicate that over-expression of *SibHLH137* significantly promotes anthocyanin biosynthesis and accumulation in foxtail millet, which may be closely associated with the transcriptional activation of late anthocyanin biosynthetic pathway genes, particularly *SiDFR*.

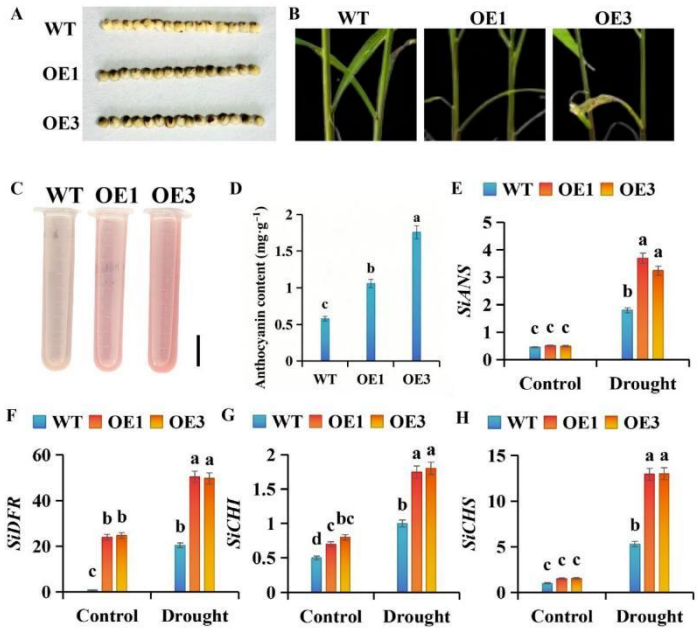



**Figure 11.** Phenotypes of foxtail millet over-expressing *SibHLH137*. (A)Phenotypes of hulled and dehulled grains of WT, OE1, OE3 and OE4. (B)Stem color of WT, OE1 and OE3. (C)Color comparison of anthocyanin extracts from whole plants of WT, OE1 and OE3. (D)Determination of total anthocyanin content in WT and over-expression lines. (E-H)Relative expression levels of anthocyanin biosynthetic genes under normal and drought conditions. . Scale bars represent 2.5 mm. Different lowercase letters indicate significant differences ($P < 0.05$).

## 3.5 Over-expression of *SibHLH137* Enhances Drought Tolerance and Antioxidant Capacity in Foxtail Millet

### 3.5.1 Over-expression of *SibHLH137* Enhances Osmotic and Drought Stress Tolerance in Foxtail Millet

To evaluate the function of *SibHLH137* in drought stress response, two over-expression lines (OE1 and OE3) were selected for osmotic and drought stress treatments. After 5 d of PEG-6000-simulated osmotic stress, wild-type (WT) plants exhibited severe wilting and leaf curling, whereas over-expression lines showed significantly milder wilting with only partial leaf shrinkage. Following 7 d of rewatering, OE lines recovered rapidly (Figure 12A). Physiological measurements revealed no significant difference in relative water content between WT and OE lines under control conditions; however, after stress treatment, relative water content decreased in all lines, but OE lines maintained significantly higher levels than WT (Figure 12B). Meanwhile, proline content in OE lines accumulated substantially under stress conditions, significantly exceeding that of WT (Figure 12C). After 7 d of rewatering, the survival rates of OE1 and OE3 were significantly higher than that of WT (Figure 12D). Following 7 d of soil drought treatment, most leaves of WT plants dried and wilted, whereas OE lines only showed yellowing in lower leaves while remaining largely green and upright. After rewatering, OE lines recovered rapidly, whereas WT recovered slowly (Figure 12E), with survival rates of OE1 and OE3 significantly higher than that of WT (Figure 12F). Leaf water loss rate measurements showed that OE lines exhibited significantly lower water loss rates throughout the entire measurement period compared to WT, indicating that over-expression of *SibHLH137* contributes to maintaining leaf water retention capacity (Figure 12G). Collectively, these results demonstrate that over-expression of *SibHLH137* significantly enhances tolerance to both osmotic and drought stress in foxtail millet.

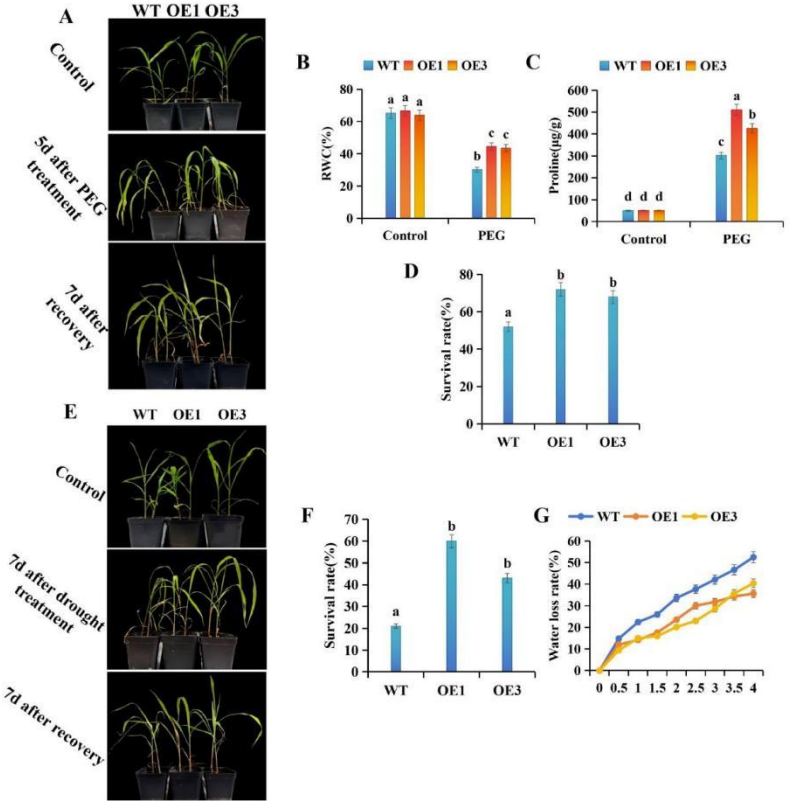



**Figure 12.** Analysis of osmotic and drought stress tolerance in transgenic foxtail millet plants overexpressing *SibHLH137*. (A)Phenotypes of wild-type (WT) and over-expression lines (OE1, OE3) under 23% (w/v) PEG-6000 treatment for 5d and recovery for 7d. (B)Relative water content. (C)Proline content. (D)Survival rate after 7d of recovery from PEG treatment. (E)Phenotypes of WT and OE lines under soil drought treatment for 7d and recovery for 7d. (F)Survival rate after 7d of recovery from soil drought. (G)Leaf water loss rate. Different lowercase letters indicate significant differences ($P < 0.05$).

### 3.5.2 Over-expression of *SibHLH137* Enhances Antioxidant Capacity in Foxtail Millet

Under drought stress conditions, the activities of superoxide dismutase (SOD), catalase (CAT), and peroxidase (POD) were significantly elevated in OE lines. SOD activity increased by 108.3% and 135%, CAT activity by 164.14% and 119.03%, and POD activity by 115.38% and 125.81% in OE1 and OE3, respectively, with the increases being substantially higher than those in wild-type (WT) plants (76.1%, 43.17%, and 100%, respectively; Figures 13A-C). Drought stress induced an increase in malondialdehyde (MDA) content and triggered the accumulation of superoxide anion ($O_2^-$) and hydrogen peroxide ($H_2O_2$) in all lines; however, the accumulation levels of these oxidative damage indicators were significantly lower in OE lines than in WT. Further analysis indicated that the significant upregulation of antioxidant enzyme activities in OE lines effectively suppressed the excessive accumulation of $O_2^-$ and $H_2O_2$, and reduced the level of MDA, a product of membrane lipid peroxidation, thereby alleviating drought-induced oxidative damage (Figures 13D-H). Collectively, these results suggest that *SibHLH137* may enhance drought stress tolerance by positively regulating the antioxidant enzyme system, consequently mitigating physiological damage caused by oxidative stress.

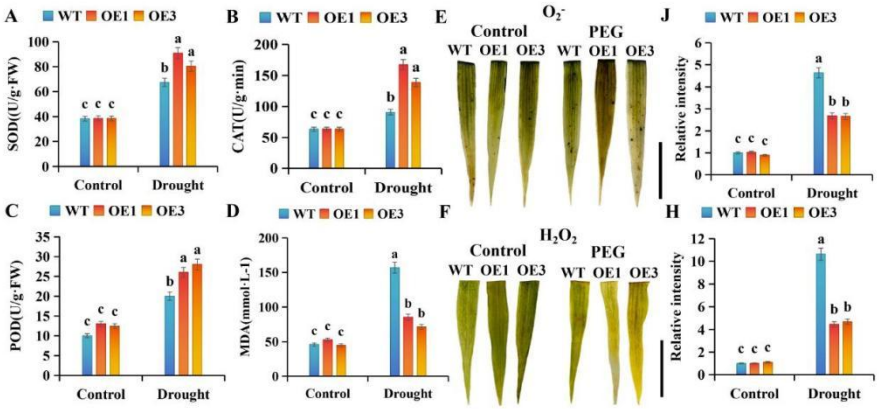



**Figure 13.** Analysis of antioxidant enzyme activities and ROS accumulation in response to drought stress. (A-C)Activities of SOD, CAT and POD. (D)MDA content. (E)DAB staining for $H_2O_2$ accumulation. (F)NBT staining for $O_2^-$ accumulation. Scale bars = 2 cm. (G-H) Relative staining intensity of $H_2O_2$ and $O_2^-$. Scale bars represent 2 cm. Different lowercase letters indicate significant differences ($P < 0.05$).

### 3.6 *SibHLH137* Regulates the Expression of Drought-Responsive Genes

To investigate the molecular mechanism by which *SibHLH137* enhances drought tolerance in foxtail millet, the transcript levels of multiple drought-responsive genes were examined by qRT-PCR in wild-type (WT) and over-expression lines (OE1, OE3) under drought stress. After 5h of drought treatment, the transcript levels of *SiDREB2* and *SiRAB18* increased, with higher levels in OE lines than in WT; the transcript levels of *SiNCED1*, *SiATG8a*, and *SiNAC110* also increased significantly ($P < 0.05$), and were higher in OE lines (Figures 14A-E). After 24h of drought treatment, the transcript levels of SiLEA14, SiGRF1, and SiYTH1 increased substantially, with significantly higher expression in OE lines than in WT ($P < 0.05$) (Figures 14F-H). These results indicated that *SiDREB2*, *SiNCED1*, *SiRAB18*, *SiATG8a*, and *SiNAC110* were induced at the early stage (5h) of drought stress, with higher expression levels in the over-expression lines. Moreover, other stress-responsive genes (*SiLEA14*, *SiGRF1*, and *SiYTH1*) exhibited similar expression patterns after 24h of stress treatment, being more strongly induced in *SibHLH137*-overexpressing plants. This suggests that *SibHLH137* may enhance stress tolerance by upregulating these key stress-responsive genes.

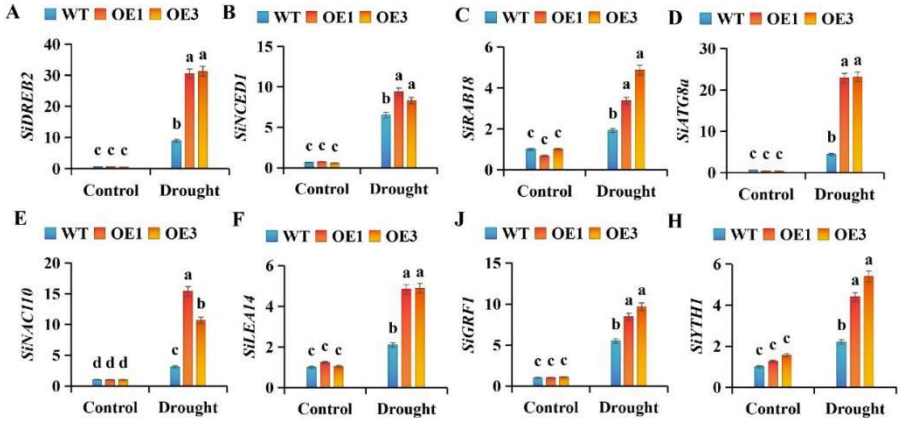



**Figure 14.** Analysis of stress-responsive genes in transgenic millet and wild-type (WT) plants. Total RNA was extracted from leaves of plants subjected to drought treatment for 5h and 24h, with untreated plants serving as the control. Using cDNA templates from the 5h drought-treated samples, the relative expression levels of stress-related genes *SiDREB2* (A), *SiNCED1* (B), *SiRAB18* (C), *SiATG8a* (D), and *SiNAC110* (E) were analyzed by qRT-PCR. Using cDNA templates from the 24h drought-treated samples, the relative expression levels of *SiLEA14* (F), *SiGRF1* (G), and SiYTH1 (H) were analyzed. Different lowercase letters indicate significant differences ($P < 0.05$).

### 3.7 Promoter Cis-Acting Element Analysis of Differentially Expressed Genes in *SibHLH137*-Overexpressing Foxtail Millet

The qRT-PCR analysis above revealed that the expression levels of multiple genes were significantly higher in transgenic plants than in wild-type plants, including the anthocyanin biosynthesis-related genes SiCHI, SiCHS, SiDFR, and SiANS, as well as the stress-responsive genes *SiDREB2*, *SiNCED1*, *SiRAB18*, *SiATG8a*, *SiLEA14*, *SiGRF1*, *SiYTH1*, and *SiNAC110*.

Both CACGTT and CACGTC are atypical G-box variants of the E-box (CANNTG) family, which typically interact with MYC-type, PIF-type, and anthocyanin-related bHLH proteins, participating in anthocyanin biosynthesis, ABA/drought responses, and light signal regulation. Promoter sequence analysis of these 12 potential downstream target genes was performed using the PlantCARE database. Among the 12 differentially expressed genes, eight promoters (anthocyanin biosynthesis-related genes SiCHS and SiDFR; stress-responsive genes *SiDREB2*, *SiNCED1*, *SiRAB18*, *SiATG8a*, *SiGRF1*, and *SiYTH1*) were found to contain 1–4 G-box cis-acting elements in their promoter regions (Figure 15).

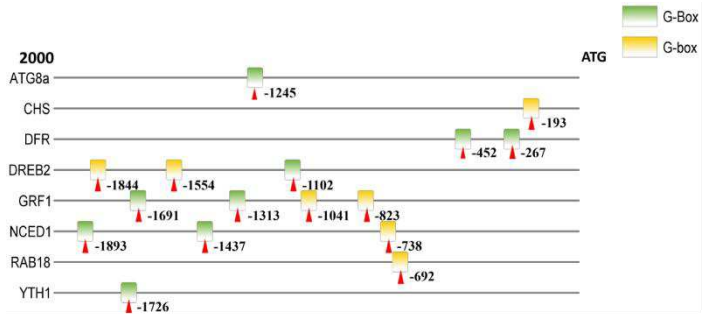



**Figure 15.** Promoter analysis of downstream target genes of *SibHLH137*. Note: Red triangle: G-box component; : CACGTT; : CACGTC.

## 4. Discussion

### 4.1 *SibHLH137* Positively Regulates Anthocyanin Biosynthesis

Anthocyanin accumulation in plants is finely regulated by the MYB-bHLH-WD40 (MBW) transcriptional complex, in which bHLH transcription factors interact with MYB proteins to cooperatively activate the expression of anthocyanin biosynthetic structural genes (Zhang et al., 2023). In this study, over-expression of *SibHLH137* significantly deepened the pigmentation of foxtail millet caryopses and stems, and markedly increased total anthocyanin content compared with wild-type plants. The transcript levels of anthocyanin biosynthesis-related genes *SiCHI*, *SiCHS*, *SiDFR*, and *SiANS* were all significantly upregulated, with *SiDFR* expression reaching up to 30-fold that of the wild type. This result suggests that *SibHLH137* may serve as a positive regulator of the anthocyanin biosynthetic pathway in foxtail millet, particularly exerting a strong transcriptional activation effect on *SiDFR*. DFR (dihydroflavonol 4-reductase) catalyzes the reduction of dihydroflavonols to leucoanthocyanidins and is widely recognized as a key rate-limiting enzyme in the anthocyanin biosynthetic pathway (Lo et al., 2006). As a "late" step in anthocyanin synthesis, DFR is positioned at a metabolic branch point, and its activity directly influences the final accumulation levels of anthocyanin products. Studies across different plant species have consistently demonstrated that the regulation of DFR expression is a critical determinant of anthocyanin biosynthesis (Tao et al., 2024). For instance, in rice, the bHLH binding site in the DFR promoter region has been shown to be essential for its expression (ElShamey et al., 2025; Lee et al., 2023); in citrus, differential DFR expression between blood orange and common orange directly accounts for the presence or absence of anthocyanin accumulation (Sicilia et al., 2020). Drought stress further intensified the purple coloration of stems in overexpression lines and concurrently induced 2- to 3-fold upregulation of the aforementioned structural genes. This phenomenon is highly consistent with recent findings in Chaenomeles speciosa, where drought stress-induced *CsbHLH111* interacts with *CsMYB123* to cooperatively activate anthocyanin biosynthetic genes including *CsCHI*, *CsDFR*, and *CsANS*, thereby promoting anthocyanin accumulation (Ding et al., 2025; Wang et al., 2023). Similarly, in Glycyrrhiza uralensis, *GubHLH38* and *GubHLH64* have been confirmed to be closely associated with anthocyanin biosynthesis under abiotic stress conditions (Lira et al., 2017).

### 4.2 *SibHLH137* Enhances Drought Tolerance in Foxtail Millet Through Multifaceted Synergistic Pathways

Drought stress is one of the major environmental factors limiting crop productivity. Plants adapt to water-deficit conditions by accumulating osmotic regulatory substances, enhancing antioxidant capacity, and modulating the expression of stress-responsive genes. In this study, the *SibHLH137* over-expression lines exhibited significantly higher relative water content, substantially greater proline accumulation, and markedly lower malondialdehyde (MDA) content compared with wild-type plants under drought stress. These results indicate that *SibHLH137* enhances drought tolerance in foxtail millet by promoting the accumulation of osmotic regulatory substances and alleviating membrane lipid peroxidation damage. Osmotic adjustment is a key physiological mechanism by which plants cope with drought stress, and proline, as an

important compatible solute, not only contributes to osmotic potential maintenance but also functions in reactive oxygen species (ROS) scavenging and protein stability protection (Huang et al., 2019). Similarly, over-expression of *MdbHLH104* in apple was reported to enhance tolerance to abiotic stress, and its mechanism was also associated with the strengthening of the ROS scavenging system (Wu et al., 2026).

The expression of multiple drought-responsive genes was significantly altered in *SibHLH137* over-expression lines. Notably, *SiDREB2*, which encodes a dehydration-responsive element-binding protein, has been demonstrated to activate the expression of multiple downstream drought tolerance genes in species such as *Arabidopsis* (Le et al., 2026). The enhanced induction of *SiDREB2* expression in the *SibHLH137* over-expression background suggests that *SibHLH137* may function upstream of DREB2 in drought signal transduction. Promoter analysis revealed that the promoter regions of *SiDREB2*, *SiNCED1*, *SiRAB18*, *SiATG8a*, *SiGRF1*, and *SiYTH1* all contain 1-4 G-box elements. This observation is consistent with the report that *CsbHLH111* can directly bind to the G-box element in the *CsCHI* promoter in Chaenomeles speciosa, implying that *SibHLH137* may also exert transcriptional regulatory effects by directly targeting the promoters of these stress-responsive genes. However, bHLH transcription factors typically require interaction with MYB partners for specific DNA binding. Therefore, the interacting partners of *SibHLH137* and its regulatory network under drought stress remain to be further investigated.

### 4.3 *SibHLH137* May Serve as a Key Node Integrating Anthocyanin Biosynthesis and Drought Response

Anthocyanins not only contribute to tissue pigmentation but also function in scavenging reactive oxygen species (ROS) and protecting against photooxidative damage, thus playing important roles in drought stress adaptation. In this study, drought stress simultaneously induced anthocyanin accumulation and the expression of related structural genes, suggesting that SibHLH137-mediated anthocyanin synthesis may be a component of the drought tolerance strategy in foxtail millet. This phenomenon is similar to the mechanism in Chaenomeles speciosa, where drought-induced CsbHLH111 and *CsMYB123* synergistically activate anthocyanin biosynthesis; however, whether *SibHLH137* employs a similar MYB interaction mode remains to be verified (Shangguan et al., 2026).

In recent years, accumulating evidence has indicated that bHLH transcription factors serve as hub regulators in coordinating secondary metabolism and stress adaptation. For example, in Glycyrrhiza uralensis, bHLH transcription factors are not only involved in anthocyanin biosynthesis but also respond to abiotic stress through the jasmonic acid signaling pathway (Ai et al., 2026). In apple, *MdbHLH3* responds to temperature signals during cold-induced anthocyanin accumulation (Wang et al., 2025). In this study, the significant upregulation of *SiNCED1*, a key gene in ABA biosynthesis, and SiRAB18, an ABA-responsive gene, in SibHLH137 overexpression lines under drought stress suggests that *SibHLH137* may interact with the ABA signaling pathway. A recent study in Ziziphus jujuba reported that ABA and ethylene mediate drought-induced anthocyanin synthesis through a MYB-bHLH transcriptional cascade, providing a reference for understanding the involvement of *SibHLH137* in ABA signal transduction (Li et al., 2025).

This study preliminarily reveals the dual function of *SibHLH137* in regulating anthocyanin biosynthesis and drought stress responses. Based on the available results, we hypothesize the following working model (Figure 16): under normal growth conditions, *SibHLH137* interacts with specific MYB and WD40 transcription factors to bind to G-box elements in the promoters of downstream target genes (such as *SiDFR* and *SiCHS*), thereby activating the anthocyanin biosynthetic pathway. Under drought stress conditions, the expression or activity of *SibHLH137* is further enhanced, which on one hand intensifies anthocyanin synthesis to scavenge drought-induced ROS, and on the other hand activates stress-responsive genes including *DREB2* and *NCED1*, thereby enhancing drought tolerance in foxtail millet. Future studies employing techniques such as DNA affinity purification sequencing (DAP-seq), chromatin immunoprecipitation (ChIP), and yeast two-hybrid library screening will be valuable for systematically identifying the direct target genes and interacting proteins of SibHLH137, thereby providing further evidence for the elucidation of its molecular regulatory network.

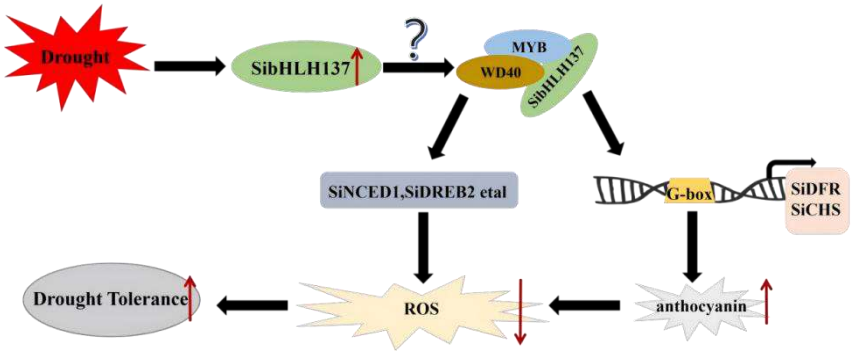



**Figure 16.** Hypothetical working model of the *SibHLH137* gene.

**Supplementary Materials:** Table S1 The callus induction rates of Heizhigu, Heigu, Xiaoheigu, and CC431 in four different culture media. Table S2 Effect of different concentrations of 6-BA and NAA on the differentiation of mature embryos. Table S3 Effects of NAA rooting media at different concentrations on the rooting of cluster shoots. Table S4 Primer sequences. Table S5 Medium formula. Figure S1 Genotype screening and medium optimization for in vitro regeneration from mature embryos of foxtail millet.

**Author Contributions:** MPZ provided the material and designed the experiment. XY, MJK, and LZ prepared the draft of the manuscript. XY, MJK, and LZ performed the experiments. YJS provided detection and analysis of various indicators. XQF analyzed the data. All authors read and approved the final manuscript.

**Data Availability Statement:** The original contributions presented in this study are included in the article/supplementary material. Further inquiries can be directed to the corresponding author(s).

**Acknowledgments:** This work was supported by the Yuncheng Salt Lake Protection and Utilization Research Institute of Shanxi(YHYJ-2023003) and 2025 Shanxi "Three Regions" Science and Technology Talent Support Program(Jin Cai Jiao (2025) No. 106).

**Conflicts of Interest:** The authors declare that they have no confict of interest.

## References

1. Ai C, Wang L, Luo Z, Wang Y, Zhao X, Wang L, Sun J, Lv K, Yan X, Cao H, Muhammad N, Zhang Q, Liu M, Liu Z. Molecular Mechanism of ZjWRKY40-zju-miR157 Module Regulating Phytoplasma Tolerance in Jujube[J]. Mol Plant Pathol. 2026, 27(2): e70219.
2. Cui B. Mechanism of salt tolerance regulation by calmodulin-like gene *SsCML48* in Suaeda salsa[D]. Jinan: Shandong Normal University, 2023.
3. Ding G, Shi Y, Xie K, Li H, Xiao G. Genome-wide identification and expression analysis of bHLH gene family revealed their potential roles in abiotic stress response, anthocyanin biosynthesis and trichome formation in Glycyrrhiza uralensis[J]. Front Plant Sci. 2025, 15: 1485757.
4. ElShamey EA, Yang X, Yang J, Pu X, Yang L, Ke C, Zeng Y. Occurrence, Biosynthesis, and Health Benefits of Anthocyanins in Rice and Barley. Int J Mol Sci. 2025 Jun 27;26(13):6225.
5. Hao G, Edwards J, Rhoades N, McCormick SP. *Arabidopsis thaliana* detoxification gene *AtDTX1* is involved in trichothecene 3-acetyl-deoxynivalenol efflux[J]. Front Plant Sci. 2025, 16: 1574367.
6. Hou ZH, Zheng WJ, Zheng L, Wang JY, Zhang SX, Wei JT, Yang SH, Jiao YC, Cheng WJ, Yu TF, Ma XF, Ru JN, Liu YW, Cao XY, Chen J, Zhou YB, Chen M, Li LH, Ma YZ, Nie XJ, Xu ZS. TaPPR13, a Pentatricopeptide Repeat Protein Gene Activated by *TaBZR2*, Confers Drought Stress Tolerance by Enhancing the Antioxidant Defense System and Promoting Retrograde Signaling in Wheat (*Triticum aestivum*)[J]. Adv Sci (Weinh). 2025, 12(36): e02984.
7. HUANG S, ZHANG A, JIN J B, et al. *Arabidopsis* histone H3K4 demethylase JMJ 17 functions in dehydration stress response [J]. New Phytologist. 2019, 223(3): 1372-87.
8. Jiang M, Xu Z, Zheng F, et al. Identification and expression analysis of *ALDH* gene family in Rubus chingii[J]. Journal of Nuclear Agricultural Sciences, 2026, 40(3): 433-444.
9. Le Y, Chen M, Zhu D, Xu Z, Fu C, Xiong X, Li Y, Yang N, Hui L, Zhang X, Lin Z. Transcriptional Regulation of *SWEET15_A01* by MYB44/bHLH3 Modulates Carbon Allocation in Cotton Ovule and Fibre to Affect Seed and Fibre Traits[J]. Plant Biotechnol J. 2026, 24(3):

1769-1791.
10．Lee C, Lee YS, Hong HC, Hong WJ, Koh HJ, Jung KH. Reinterpretation of anthocyanins biosynthesis in developing black rice seeds through gene expression analysis. PLoS One. 2023 Jun 2;18(6):e0286539.
11．Li D, Wang H, Jia L, et al. Research progress on anthocyanin biosynthesis and regulatory mechanism of *DFR* gene in plants[J]. China Vegetables, 2025, (10): 45-58.
12．Li W. Cloning and functional study of *SiSERK1* gene in foxtail millet[D]. Lanzhou: Northwest Normal University, 2022.
13．Li Y, Chen Y, Wu K, et al. Cloning of tomato *AP2a* and *MYB12* transcription factors and their expression analysis under *CYRSV* infection[J]. Guihaia, 2025: 1-15.
14．Liang Z, Wang N, Xu C, et al. Effects of PRD and nitrogen forms on free amino acid and proline contents in rice[J]. Journal of Shaanxi Agricultural Sciences, 2026, 72(1): 17-23+31.
15．Lira BS, Gramegna G, Trench BA, Alves FRR, Silva EM, Silva GFF, Thirumalaikumar VP, Lupi ACD, Demarco D, Purgatto E, Nogueira FTS, Balazadeh S, Freschi L, Rossi M. Manipulation of a Senescence-Associated Gene Improves Fleshy Fruit Yield[J]. Plant Physiol. 2017, 175(1): 77-91.
16．Liu L, Qi S, Xu X. Effects of exogenous melatonin on growth and physiological characteristics of *Petunia hybrida* under salt stress[J/OL]. Shandong Agricultural Sciences, 2026: 1-11.
17．Lo Piero AR, Puglisi I, Petrone G. Gene characterization, analysis of expression and in vitro synthesis of dihydroflavonol 4-reductase from [*Citrus sinensis* (L.) Osbeck][J]. Phytochemistry. 2006, 67(7): 684-95.
18．Prakash R, Idowu O, Holzapfel B, Zhang X, Smith JP, Ashnest JR. Role of non-structural carbohydrates in the sustainable production of apples （Malus domestica）[J]. Funct Plant Biol. 2026, 53(3): FP25232.
19．Ren Y, Zhang S, Zhao Q, Wu Y, Li H. The *CsMYB123* and *CsbHLH111* are involved in drought stress-induced anthocyanin biosynthesis in *Chaenomeles speciosa*[J]. Mol Hortic. 2023, 3(1): 25.
20．Shangguan X, Liu H, Li H, Zhang H, Li J, Chen Z. A BAHD acyltransferase of cotton affects plant drought tolerance and yield by regulating cuticle formation and cuticle permeability[J]. Plant Sci. 2026, 365: 113014.
21．Sicilia A, Scialò E, Puglisi I, Lo Piero AR. Anthocyanin Biosynthesis and DNA Methylation Dynamics in Sweet Orange Fruit [*Citrus sinensis* L. (Osbeck)] under Cold Stress. J Agric Food Chem. 2020 Jul 1;68(26):7024-7031.
22．Song X, Wei J, Di S, et al. Research progress on regulatory mechanisms of anthocyanin transcription factors and metabolic engineering[J]. Chinese Bulletin of Botany, 2019, 54(1): 133-156.
23．Tao H, Gao F, Linying Li, He Y, Zhang X, Wang M, Wei J, Zhao Y, Zhang C, Wang Q, Hong G. *WRKY33* negatively regulates anthocyanin biosynthesis and cooperates with *PHR1* to mediate acclimation to phosphate starvation[J]. Plant Commun. 2024, 5(5): 100821.
24．Wang MJ, Ou Y, Li Z, Zheng QD, Ke YJ, Lai HP, Lan SR, Peng DH, Liu ZJ, Ai Y. Genome-Wide Identification and Analysis of bHLH Transcription Factors Related to Anthocyanin Biosynthesis in *Cymbidium ensifolium*[J]. Int J Mol Sci. 2023, 24(4): 3825.
25．Wang S, Xiao X, Dou Q, et al. Cloning and subcellular localization analysis of GGPPS from *Bletilla striata*[J]. Journal of Agricultural Biotechnology, 2025, 33(11): 2404-2413.
26．Wang W, Cui Q, Qiu S. Effect of wind load on stem deformation of individual foxtail millet plants[J]. Journal of Shanxi Agricultural University (Natural Science Edition), 2024, 44(6): 99-106.
27．Wu L, Qu L. Research progress on nutritional functional properties and processing of foxtail millet[J]. Food Research and Development, 2018, 39(15): 191-196.
28．Wu Y, Liu Q, Yan X, Kato Y, Tanaka M, Inokuchi S, Yoshizawa T, Morohashi S, Kijima H. [Corrigendum] Podoplanin mediated TGF β induced epithelial mesen chymal transition and its correlation with bHLH transcription factor DEC in TE 11 cells[J]. Int J Oncol. 2026, 68(4): 41.
29．Zhang B, Huang ZY, Wang ZD, Li GF, Hu GB, Yang YZ, Zhao ZY. Jasmonate-responsive MdMYC2/MdMED25 complex regulates malic acid accumulation in apples through the *miR858-MdMYB73* module[J]. J Integr Plant Biol. 2026, 68(1): 148-168.
30．Zhang D, Zhang X, Li J, et al. Effects of drought stress on physiological characteristics of *Glycyrrhiza uralensis* seedlings[J]. Current Biotechnology, 2026, 16(1): 86-93.
31．Zhang S, Ren Y, Zhao Q, Wu Y, Zhuo Y, Li H. Drought-induced *CsMYB6* interacts with *CsbHLH111* to regulate anthocyanin biosynthesis in

530 *Chaenomeles speciosa*[J]. Physiol Plant. 2023, 175(1): e13859.
531
532

## Supplementary Files

This is a list of supplementary files associated with this preprint. Click to download.

- SupplementaryMaterials.docx